JCS ePress online publication date 11 March 2008

PGE_2-mediated podosome loss in dendritic cells is dependent on actomyosin contraction downstream of the RhoA–Rho-kinase axis

Suzanne F. G. van Helden[1], Machteld M. Oud[1], Ben Joosten[1], Niels Peterse[2], Carl G. Figdor[1,*] and Frank N. van Leeuwen[2]

[1]Department of Tumor Immunology and [2]Laboratory of Pediatric Oncology, Nijmegen Centre for Molecular Life Sciences, Radboud University Nijmegen Medical Centre, PO Box 9101, 6500 HB Nijmegen, The Netherlands

*Author for correspondence (e-mail: c.figdor@ncmls.ru.nl)

Accepted 16 January 2008
Journal of Cell Science 121, 1096-1106 Published by The Company of Biologists 2008
doi:10.1242/jcs.020289

Summary

Podosomes are dynamic adhesion structures found in dendritic cells (DCs) and other cells of the myeloid lineage. We previously showed that prostaglandin E2 (PGE_2), an important proinflammatory mediator produced during DC maturation, induces podosome disassembly within minutes after stimulation. Here, we demonstrate that this response is mediated by cAMP elevation, occurs downstream of Rho kinase and is dependent on myosin II. Whereas PGE_2 stimulation leads to activation of the small GTPase RhoA, decreased levels of Rac1-GTP and Cdc42-GTP are observed. These results show that PGE_2 stimulation leads to activation of the RhoA–Rho-kinase axis to promote actomyosin-based contraction and subsequent podosome dissolution. Because podosome disassembly is accompanied by de novo formation of focal adhesions, we propose that the disassembly/formation of these two different adhesion structures is oppositely regulated by actomyosin contractility and relative activities of RhoA, Rac1 and Cdc42.

Supplementary material available online at
http://jcs.biologists.org/cgi/content/full/121/7/1096/DC1

Key words: Dendritic cell, PGE_2, Podosomes, Actomyosin contraction, RhoA

Introduction

Based on stability, composition and subcellular localization, different classes of cell-matrix adhesions can be recognized. In most cell types, focal adhesions (FAs), which are present at the end of actin stress fibres, are the most prominent. However, cells of the myeloid lineage – such as macrophages, osteoclasts and dendritic cells (DCs) – form podosomes, specialized punctuate adhesions clearly distinct from FAs (Linder and Aepfelbacher, 2003). Podosomes consist of an actin-dense core surrounded by a ring of cytoskeletal proteins also present in FAs, such as vinculin, paxillin and talin, known to connect integrins to the actin cytoskeleton (Buccione et al., 2004). Unlike FAs, podosomes are sites of active matrix degradation that promote cell migration and invasion, although, in osteoclasts, they have a more specialized role in bone resorption (Buccione et al., 2004). Moreover, it has been suggested that podosomes facilitate transendothelial migration (Calle et al., 2006; Carman et al., 2007).

DCs are highly specialized antigen-presenting cells that play a central role in the induction of T-cell-mediated immunity. In response to antigen uptake and exposure to inflammatory stimuli, DCs undergo a dramatic phenotypic conversion from a tissue-resident, antigen-capturing cell to a highly migratory antigen-presenting cell, a process known as DC maturation (Banchereau and Steinman, 1998). Not surprisingly, this transition is accompanied by extensive changes in cell adhesion and cytoskeletal organization (Burns et al., 2004; De Vries et al., 2003a; West et al., 2004). A prominent feature of immature DCs (iDCs), which strongly interact with the extracellular matrix, is the presence of podosomes (Burns et al., 2004; Van Helden et al., 2006). By contrast, mature DCs (mDCs), which are loosely adherent (Burns et al., 2004), no longer form podosomes on fibronectin (FN) and instead display characteristic actin-rich extensions (dendrites) that maximize the contact area for T-cell interactions (Mellman et al., 1998). Although podosomes are generally considered a feature of migratory and invasive cells, migration speeds in (podosome-bearing) iDCs are tenfold lower than those observed in mDCs (Van Helden et al., 2006). The migratory capacity of DCs on FN in vitro correlates well to the migratory capacity in vivo and the high-speed migration is essential for efficient induction of immune responses in cancer patients treated with DC vaccination (De Vries et al., 2003a). The presence of podosomes appears to be incompatible with the high-speed migration observed in mDCs, which could explain why these structures are lost during DC maturation.

Podosomes are influenced by both actin and microtubule dynamics (Burns et al., 2001; Linder and Aepfelbacher, 2003), and are regulated by coordinated activity of the Rho GTPases Rho, Rac and Cdc42 (Burns et al., 2001). However, the mechanisms that lead to podosome formation/dissolution are still poorly understood. Previously, we found that stimulation of iDCs with maturation-inducing agents, such as lipopolysaccharide, leads to a loss of podosomes and that this response is dependent on the production of prostaglandins by the DCs (Van Helden et al., 2006). Moreover, addition of prostaglandin E2 (PGE_2) was sufficient to induce podosome dissolution within minutes after stimulation. These results illustrate that (early) DC maturation involves extensive changes in cytoskeletal organization and cell adhesion, which requires coordinate interactions between signalling

molecules, integrins and the actomyosin cytoskeleton. Because PGE_2 plays a key role in the DC maturation process (De Vries et al., 2003b; Legler et al., 2006) and little is known about the signal-transduction pathways responsible for cytoskeletal remodelling during DC maturation, we have examined in detail how PGE_2 signalling affects podosome turnover in DCs.

Results

iDCs rapidly dissolve podosomes and form FAs in response to PGE_2 stimulation

Immature DCs, seeded on FN, form prominent podosomes. We have shown that PGE_2 causes a nearly complete dissolution of podosomes (from 89±1% in the control situation to 10±2% of the DCs displaying podosomes after 5 minutes of PGE_2 stimulation) within minutes after stimulation, an effect that is maintained in the continued (16 hours) presence of PGE_2 (Fig. 1A-D). In addition, in part of the DCs, we observed adhesion structures mostly at the cell periphery (Fig. 1A), which either represented FAs or (more-peripherally located) precursors of FAs known as focal complexes (Zamir and Geiger, 2001). Podosome dissolution in response to PGE_2 was accompanied by rapid de novo formation of these structures (from 56±3% in the control situation to 84±2% of the DCs displaying FAs after 5 minutes of PGE_2 stimulation) (Fig. 1A,B). The cytoskeletal protein zyxin, an established marker for mature FAs (Zaidel-Bar et al., 2003), was prominently present both in podosome rings as well as in the newly formed adhesion structures (Fig. 1C), suggesting that the latter represent FAs rather than focal complexes. After prolonged exposure to PGE_2, the amount of cells displaying FAs gradually decreased (Fig. 1A,B).

The transition from podosomes to FAs was further confirmed using interference reflection microscopy (IRM). In iDCs, podosomes were seen as dark dots and in part of the cells FAs were visible as dark stripes (Fig. 2A,B, and Movies 1, 2 and Fig. S1A in the supplementary material). Immunofluorescence detection of F-actin (staining the podosome core) and vinculin (to reveal the podosome ring as well as FAs) was used to confirm that these IRM patterns accurately detect podosomes and FAs in these cells (Fig. 2A). In some DCs, we observed bundles of actin filaments, stress fibres, connected to the FAs (Fig. 2A, lower panel). The average size of the dark spots (0.75 μm) closely corresponds to the average size of the actin core (0.78 μm), whereas the vinculin ring was slightly larger (0.91 μm) (Fig. 2C-F and Fig. S1A in supplementary material), suggesting that the structures observed with IRM represent the actin cores of the podosomes.

By live-cell imaging of iDCs using IRM, we determined that podosomes dissolve within minutes after stimulation with PGE_2, while FAs are forming within the same time frame (Fig. 2B and Movies 1, 2 in the supplementary material). In addition, stimulation with PGE_2 appeared to induce a contractile response, which can be seen in the DIC part of the movies (Movies 1, 2 in the supplementary material). IRM imaging revealed that podosome dissolution was consistently preceded by the appearance of bright rings surrounding the podosome cores (Fig. 2B and Movies 1, 2 in the supplementary material), suggesting that changes in the podosome-ring structure precede dissolution of the actin-rich core.

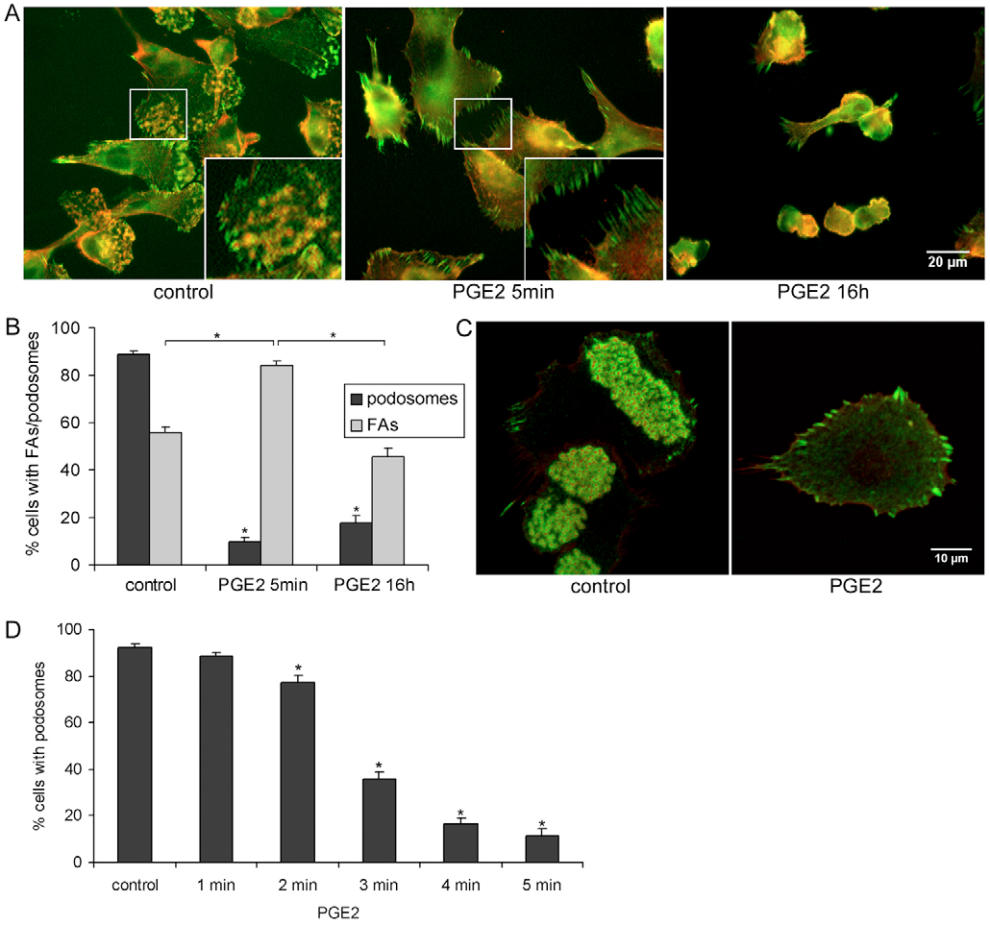

Fig. 1. PGE_2 stimulation mediated by EP2 and EP4 receptors or by cAMP elevation leads to podosome dissolution in DCs. (A-D) PGE_2 stimulation of iDCs leads to podosome loss and the appearance of FAs. (A,B) iDCs seeded on FN-coated coverslips were left untreated or were stimulated with PGE_2 for 5 minutes (min) or 16 hours (h) and stained with an anti-vinculin mAb (green) and phalloidin-Texas Red (to detect F-actin, red). (A) Representative images are depicted. (B) The number of cells displaying podosomes or FAs was counted in seven images per condition per experiment and an average (with s.e.m.) of six experiments is shown. (C) iDCs seeded on FN-coated coverslips were left untreated or were stimulated with PGE_2 for 5 minutes and stained with an anti-zyxin antibody (green) and phalloidin-Texas Red (to detect F-actin, red). (D) iDCs seeded on FN-coated coverslips were left untreated or were stimulated with PGE_2 for 1-5 minutes and stained with an anti-vinculin mAb and phalloidin-Texas Red (to detect F-actin). The number of cells displaying podosomes was determined in seven images per condition per experiment and an average (with s.e.m.) of four experiments is shown. Asterisks indicate significant differences (P<0.05).

In order to look at the onset of podosome dissolution in more detail, we fixed cells during live-cell imaging at the moment that the formation of these bright rings was apparent, followed by staining with various podosome components that either localize to the podosome ring or to the podosome core. Hence, we found that, in podosomes undergoing disassembly, as indicated by the presence of the bright rings in the IRM image, the actin core was still largely intact, whereas vinculin could no longer be detected (Fig. S1B in the supplementary material). By contrast, the podosome-ring component zyxin could still be observed in these podosomes undergoing disassembly (Fig. S1B in the supplementary material). We conclude, therefore, that the rapid loss of podosomes, induced

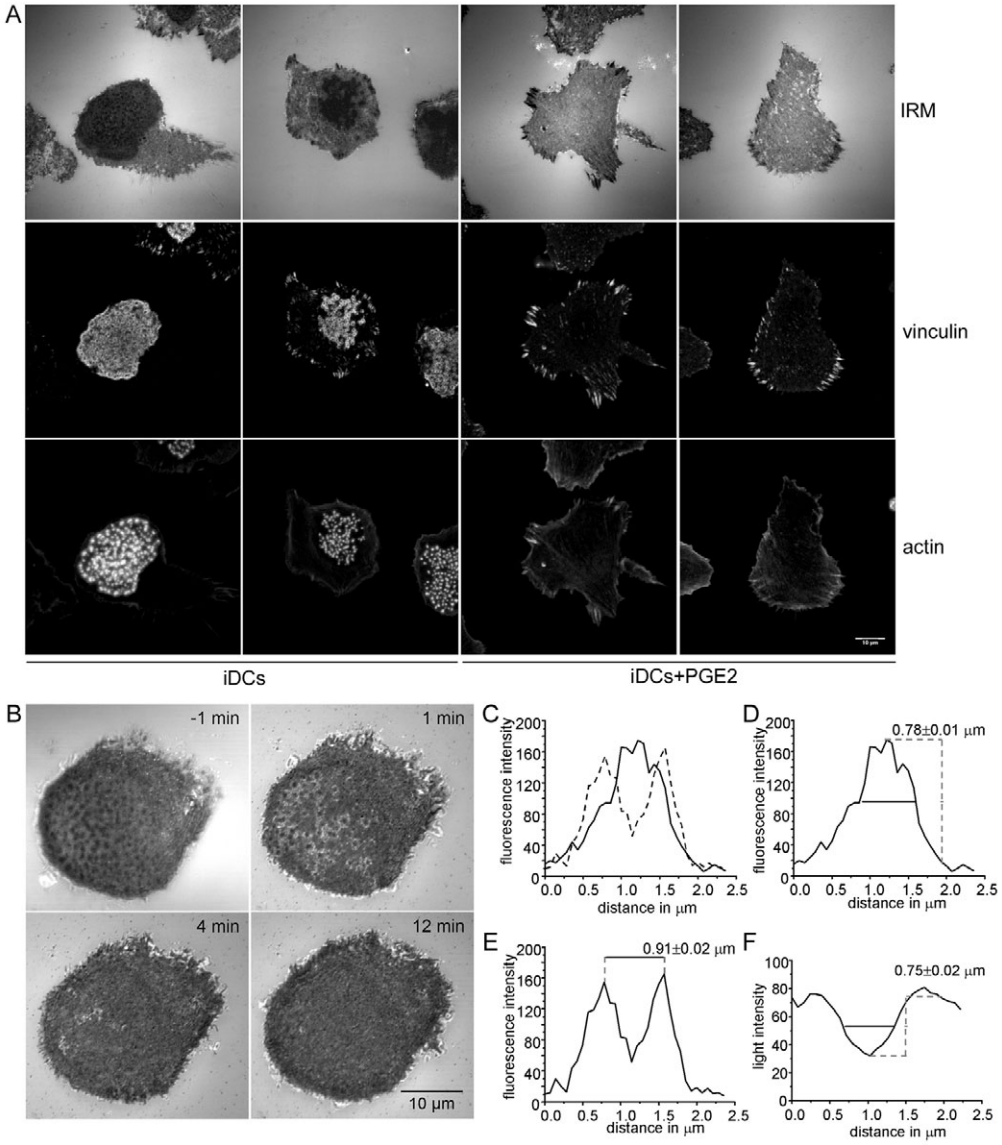

Fig. 2. Podosome loss and FA formation in DCs upon PGE_2 stimulation, visualized with IRM. Also see Movies 1, 2 and Fig. S1A,B in the supplementary material. (A) IRM images compared to fluorescent images (detected with anti-vinculin mAb, GaM-ATTO633 and phalloidin-Texas Red, to detect F-actin) identify adhesion structures as podosomes (seen as dark dots with IRM and as actin dots surrounded by vinculin rings in the fluorescent images) and FAs (seen as dark stripes with IRM and as vinculin stripes in the fluorescent images). (B) Images from an IRM movie (Movie 1 in the supplementary material) showing podosomes before stimulation (–1 min) and loss of podosomes in response to PGE_2. Note how the dissolution of podosomes is (transiently) preceded by the formation of bright rings surrounding the podosome core. FA formation in response to stimulation can be observed in the upper-right part of the images. (C) Overlay of the fluorescence intensity of the vinculin staining (broken line) and the actin staining (solid line) from straight-line selections with ImageJ through the middle of the podosome. The actin peak flanked by two vinculin peaks reflects the actin core surrounded by the vinculin-containing ring. (D-F) The size of the adhesive contacts observed by live-imaging IRM, the actin core and the vinculin ring were determined in 50 podosomes from ten different cells by making straight-line selections with ImageJ through the middle of the podosome. A representative curve of one podosome is shown and the average size is depicted in the upper-right corner of the curves with errors depicted as s.e.m. (D) The fluorescence intensity of the actin staining from a straight-line selection through the middle of a podosome. The width of the peak at half the height was used to determine the width of the actin core (0.78±0.01 µm). (E) The fluorescence intensity of the vinculin staining from a straight-line selection through the middle of a podosome. The distance from one peak to the other peak was measured to obtain the size of the vinculin ring (0.91±0.02 µm). (F) The light intensity in the IRM image from a straight-line selection through the middle of a podosome. The width of the peak at half the height was used to determine the width of the adhesive contact (0.75±0.02 µm).

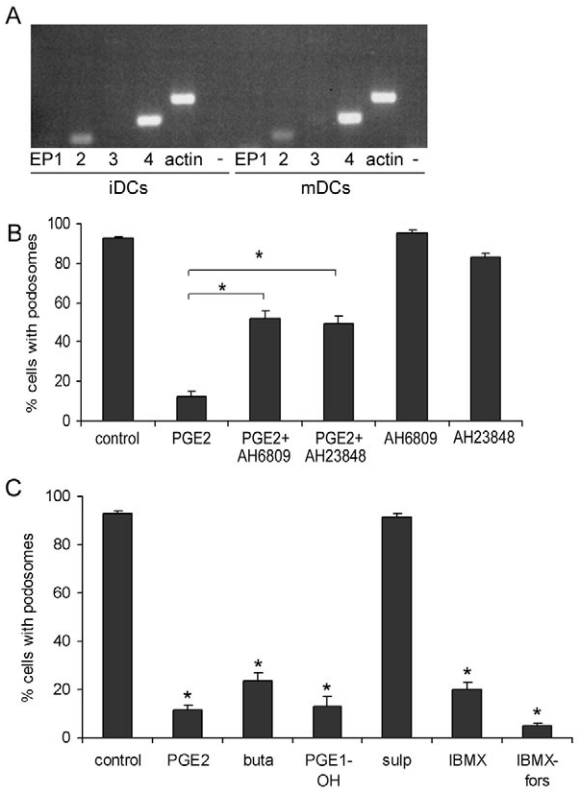

Fig. 3. PGE_2-induced podosome loss is mediated by the EP2 and EP4 receptors. (A) iDCs and mDCs express the EP2 and EP4 receptors. On iDCs and mDCs, an RT-PCR for the PGE_2 receptors EP1-EP4 was performed. Controls include β-actin (actin) and minus RT (–). A specific product is detected for EP2 and EP4 but not for EP1 and EP3 receptors. (B) EP2 and EP4 antagonists block PGE_2-induced podosome dissolution. iDCs seeded on FN-coated coverslips were left untreated or were stimulated with PGE_2 in the presence or absence of AH6809 (5 μM for 30 minutes) or AH23848 (50 μM for 30 minutes), or with AH6809 or AH23848 alone, and stained with anti-vinculin mAb and phalloidin-Texas Red (to detect F-actin). The number of cells displaying podosomes was counted in seven images per condition per experiment and an average (with s.e.m.) of four experiments is shown. (C) EP2 and EP4 agonists and cAMP elevation mimic PGE_2 in inducing podosome dissolution. iDCs seeded on FN-coated coverslips were left untreated or were stimulated with PGE_2, butaprost (buta, 2 μM for 15 minutes), PGE_1-OH (5 μg/ml for 30 minutes), sulprostone (sulp, 2 μM for 15 minutes), IBMX (10 μM for 15 minutes) or IBMX with forskolin (IBMX/fors, 10 μM for 15 minutes), and stained for vinculin and F-actin. The number of cells displaying podosomes was counted in seven images per condition per experiment and an average (with s.e.m.) of three experiments for the EP agonists (buta, PGE_1-OH and sulp) and seven experiments for cAMP elevation (IBMX and fors) is shown. Asterisks indicate significant differences (P<0.05).

by PGE_2 stimulation, involves the sequential loss of podosome components, accompanied by the formation of FAs.

PGE_2-induced podosome dissolution is mediated by the EP2 and EP4 receptors and can be mimicked by elevating cAMP levels

To date, four PGE_2 receptors (EP1-EP4) have been identified (Narumiya and FitzGerald, 2001). To investigate which PGE_2 receptors are expressed in DCs, we analyzed expression of these receptors by reverse transcriptase (RT)-PCR on iDCs and mDCs. Hence, we detected expression of EP2 and EP4, but not EP1 and EP3, receptors in these cells (Fig. 3A). Consistent with these observations, both AH6809 – an antagonist of EP1, EP2 and EP3 (Abramovitz et al., 2000) – and AH23848, which selectively blocks EP4 (Blaschke et al., 1996), alone had no effect on the amount of cells displaying podosomes, whereas they effectively interfered with PGE_2-induced podosome dissolution (Fig. 3B). In addition, sulprostone, a specific agonist for EP1/EP3 (Hata and Breyer, 2004), had no effect, whereas butaprost or PGE_1-OH, selective agonists for EP2 and EP4, respectively (Hata and Breyer, 2004), rapidly induced podosome dissolution (Fig. 3C). Furthermore, we observed that addition of IBMX, forskolin or a combination thereof, resulting in elevated cAMP levels, could induce podosome dissolution (Fig. 3C and data not shown).

PGE_2-mediated podosome loss is dependent on myosin IIA function

Because PGE_2 appears to induce a contractile response in DCs (as shown by DIC images, see Movies 1, 2 in the supplementary material), we further explored a role for myosin II in PGE_2-induced podosome dissolution. We determined by western blot analysis that myosin IIA is the predominant isoform expressed in human iDCs, whereas expression of myosin IIB was low and myosin IIC was undetectable (Fig. 4A). In most cells, we observed a fine punctuate pattern of myosin IIA distribution that was enriched in the podosome-ring structures or podosome-rich areas of the cell, whereas myosin IIB was nearly undetectable (Fig. 4B).

Importantly, inhibition of myosin II function, by pre-incubation with 10 μM of the myosin-II-specific inhibitor blebbistatin (Straight et al., 2003), blocked PGE_2-induced podosome loss (from 10±2% with PGE_2 to 60±4% with PGE_2 and blebbistatin) and FAs failed to develop (Fig. 4C and Movie 3 in the supplementary material). Although it has been reported that myosin II function is also required for the formation (and maintenance) of podosomes, incubation with blebbistatin had no effect on the amount of podosomes in unstimulated cells nor did it significantly affect myosin IIA distribution at the indicated concentration (Fig. 4D). Whereas, in unstimulated control cells, myosin IIA was enriched in podosome rings, in cells stimulated with PGE_2, a more fibrillar organization of myosin IIA was observed (Fig. 4D). This PGE_2-dependent reorganization of myosin IIA into fibrils was not observed when cells were pre-treated with blebbistatin. In addition, the formation of fibrillar myosin IIA coincided with the dissolution of podosomes and fibrillar myosin IIA assemblies appeared to specifically localize to those areas of the cell in which podosomes were actively dissolving (as indicated by the IRM ring structures) (Fig. S1C in the supplementary material), suggesting that an increase in myosin IIA activity contributes to podosome dissolution at these sites. Together, these findings indicate that PGE_2-mediated podosome dissolution and the subsequent formation of FAs requires myosin-II-mediated contraction.

PGE_2 stimulation activates RhoA, and reduces Rac1 and Cdc42 activity

Small GTPases of the Rho family (Rho, Rac and Cdc42) are key regulators of adhesion dynamics that control the formation and turnover of filamentous actin, as well as microtubules, and modulate myosin-II-based contractility (Burridge and Wennerberg, 2004; De la Roche et al., 2002). Therefore, we examined the effects of PGE_2 stimulation on Rho GTPase activity using GTPase pull-down assays. The number of cells needed for such experiments and the high protease activity observed in DC lysates precluded the use of primary DCs for this purpose. Instead, we used HL-60 cells, a

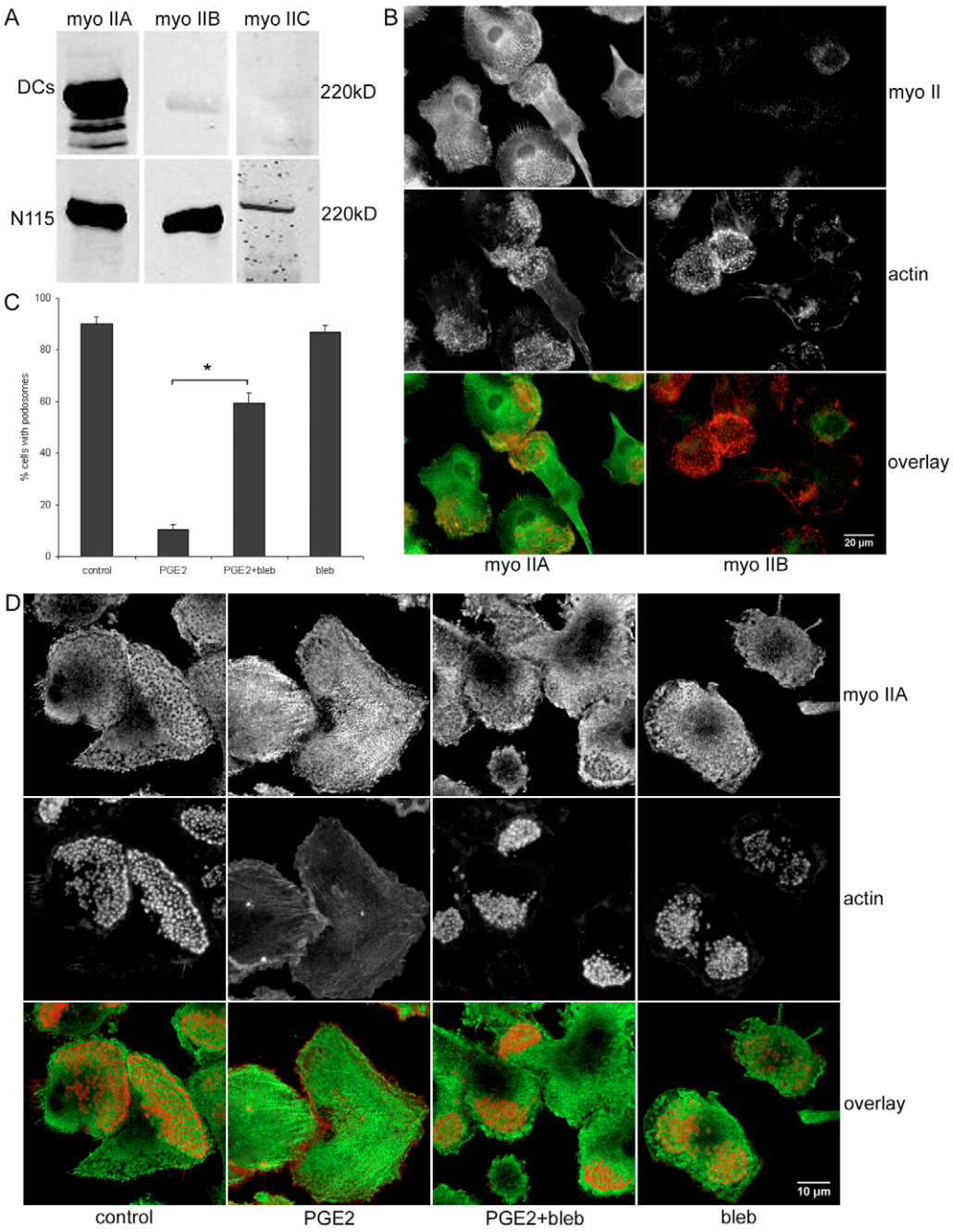

Fig. 4. Myosin II is enriched in podosomes and myosin II function is needed for PGE_2-induced podosome dissolution. (A) Myosin IIA is the predominant isoform in DCs. Cell lysates from iDCs and N1E-115 cells (N115), as a positive control that expresses all isoforms, were analyzed for expression of myosin (myo) IIA, IIB and IIC. (B) Myosin IIA is enriched in the rings of podosomes, whereas myosin IIB is nearly undetectable. iDCs were plated on FN-coated coverslips and subsequently stained with an anti-myosin-IIA or an anti-myosin-IIB antibody (green) and phalloidin-Texas Red (to detect F-actin, red). Representative images are depicted. (C) Inhibition of myosin II function blocks PGE_2-induced podosome dissolution. iDCs were plated on FN-coated coverslips and left untreated or were stimulated with PGE_2 for 5 minutes in the presence or absence of blebbistatin (bleb, 10 μM for 30 minutes), or were treated with blebbistatin alone, and stained with anti-vinculin antibodies and phalloidin-Texas Red (to detect F-actin). The number of cells displaying podosomes was counted in seven images per condition per experiment and an average (with s.e.m.) of three experiments is shown. (D) Inhibition of myosin II function blocks PGE_2-induced myosin IIA redistribution. iDCs were plated on FN-coated coverslips and left untreated or were stimulated with PGE_2 for 5 minutes in the presence or absence of blebbistatin (bleb, 10 μM for 30 minutes), or were treated with blebbistatin alone, and were stained with anti-myosin IIA antibodies and phalloidin-Texas Red (to detect F-actin). Scale bars: 20 μm (A), 10 μm (B). Asterisks indicate significant differences (P<0.05).

monocytic leukaemia cell-line that can be induced to form podosomes in response to phorbol myristic acid (PMA). We determined by RT-PCR that, similar to DCs, HL-60 cells predominantly express EP2 and EP4 receptors, and respond to PGE_2 by dissolving podosomes within the same timescale as observed in DCs. In HL-60 cells, this response appeared to be mediated primarily by the EP4 receptor, because these cells responded well to the EP4 agonist PGE_1-OH (Fig. 5), but not butaprost (data not shown).

When measuring RhoA activity, using a Rhotekin-GST fusion protein, we observed a 2.6-fold increase in RhoA-GTP levels in response to PGE_2 (Fig. 6A). We similarly determined Rac1 and Cdc42 activity in response to PGE_2 stimulation using a biotinylated Pak1 peptide. Stimulation with PGE_2 led to a decrease in Rac1 activity (to 50% of control) and a comparable decrease in Cdc42 activity (to 70% of control) (Fig. 6B,C), whereas the total amount of Rac1 and Cdc42 remained constant. These results indicate that PGE_2-induced podosome dissolution involves activation of RhoA accompanied by inactivation of Rac1 and Cdc42.

In addition, the activity of RhoA was determined upon stimulation with butaprost or PGE_1-OH, which are EP2 and EP4 agonists, respectively. Stimulation with butaprost did not change the amount of active RhoA (1.1-fold of control) (data not shown), whereas PGE_1-OH led to an increase in RhoA activity (1.6-fold of control) (Fig. 6D). These findings are consistent with our observation that PGE_2-mediated podosome dissolution in these cells appears to be predominantly mediated by EP4. Furthermore, the effect of the camp analogue 8-Bromo-cAMP on RhoA activity was investigated.

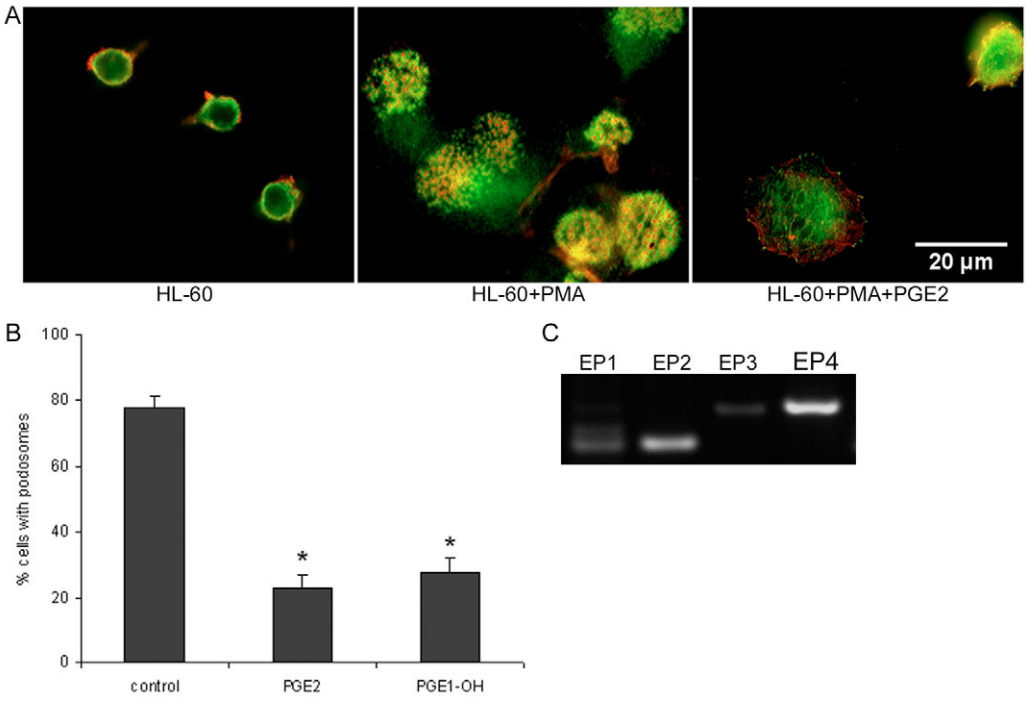

Fig. 5. HL-60 cells form podosomes upon PMA stimulation and respond to PGE_2. (A,B) HL-60 cells form podosomes upon stimulation with PMA, which dissolve after stimulation with PGE_2 or an EP4 agonist. HL-60 cells seeded on FN-coated coverslips were left untreated or were stimulated with PMA for 24 hours and then left untreated or were further stimulated with PGE_2 for 5 minutes. Cells were then stained with an anti-vinculin mAb and phalloidin-Texas Red (to detect F-actin). (A) Representative images are depicted. (B) The number of cells displaying podosomes was counted in seven images per condition per experiment and an average (with s.e.m.) of three experiments is shown. (C) HL-60 cells show expression of EP2 and EP4, whereas EP1 and EP3 receptors are nearly undetectable, as determined by RT-PCR. Asterisks indicate significant differences (P<0.05).

Hence, we determined that a 5-minute stimulation with 8-Bromo-cAMP led to a 2.5-fold increase in RhoA activity (Fig. 6E). Together, these findings suggest that raising cAMP levels, by stimulation of EP receptors, leads to activation of RhoA.

PGE_2-induced podosome dissolution is mediated by Rho kinase

We subsequently investigated a role for Rho kinase, a prominent downstream effector of RhoA, in PGE_2-induced podosome dissolution. The Rho-kinase inhibitor Y27632 (Uehata et al., 1997) effectively blocked podosome dissolution induced by PGE_2 in DCs (from 22±3% with PGE_2 to 69±5% with PGE_2 and Y27632) (Fig. 7A) as well as in HL-60 cells (data not shown). In addition, EP2- and EP4-agonist-induced podosome loss was effectively blocked by Y27632 (Fig. 7A). Podosome dissolution induced by IBMX or IBMX/forskolin was similarly blocked by Rho-kinase inhibition (from 13±5% with IBMX to 80±4% with IBMX and Y27632) (Fig. 7B). The distribution of podosomes in response to Y27632 treatment alone was unaffected, whereas, when cells were treated with Y27632 in combination with PGE_2, podosomes were still present (Fig. 7C). We conclude that PGE_2 receptors that are present on dendritic cells as well as HL-60 monocytic leukaemia cells signal to activate the RhoA–Rho-kinase axis and promote actomyosin-based contractility, leading to podosome dissolution and the formation of FAs.

Discussion

In response to antigen uptake and exposure to inflammatory stimuli, iDCs mature into highly migratory mDCs (Banchereau and Steinman, 1998). PGE_2, a proinflammatory mediator and maturation-inducing factor, is essential for the induction of full migratory capacity in DCs (Legler et al., 2006; Rubio et al., 2005; Van Helden et al., 2006; Zaidel-Bar et al., 2003). iDCs display podosomes while part of the cells also display vinculin-containing adhesions at the cell periphery. The presence of zyxin in these structures identifies these as FAs (Zaidel-Bar et al., 2003). Upon stimulation with PGE_2, iDCs rapidly dissolve podosomes and start to form FAs, suggesting that signals inducing podosome dissolution favour the formation of FAs. When, after prolonged exposure to PGE_2, the transition from strongly adhesive iDCs to highly migratory mDCs is made, the amount of cells displaying FAs gradually decreases.

Because transfection of fluorescently labelled proteins in primary DCs is difficult, we applied IRM to follow the effects of PGE_2 on DC adhesion structures in living cells. With this technique, which has been previously used to visualize either FAs or podosomes (Chou et al., 2006; Kaverina et al., 2003; Usson et al., 1997), structures close to the glass, such as podosomes and FAs, come out dark, whereas structures further away from the glass appear lighter. By combining IRM with immunofluorescence-detection after fixation, we confirmed that the dark spots observed by IRM correspond in size and localization to the actin-rich cores of podosomes. The latter might seem counter-intuitive, because the (integrin-containing) podosome rings are the primary sites for adhesion; however, the fact that podosomes are highly protrusive structures driven by actin polymerization in the core might explain why the podosome core appears closer to the glass than the surrounding ring structure (Calle et al., 2006; Carman et al., 2007; Destaing et al., 2003). Interestingly, podosome dissolution is invariably preceded by the transient appearance of bright rings in the IRM image, surrounding the actin-rich cores. By in situ fixation of podosomes undergoing dissolution, we showed that, at the time these bright rings appear, vinculin is no longer present in these podosome remnants, whereas the actin-rich cores, as well as associated zyxin, are still clearly detectable. Together, these results suggest that initial changes affect the podosome ring prior to (complete) dissolution of the actin core.

Mouse knockout studies have revealed an important role for EP4 in Langerhans cell migration (Kabashima et al., 2003), whereas, in humans, both EP2 and EP4 have been linked to DC function (Harizi et al., 2003). In line with earlier findings (Scandella et al., 2002),

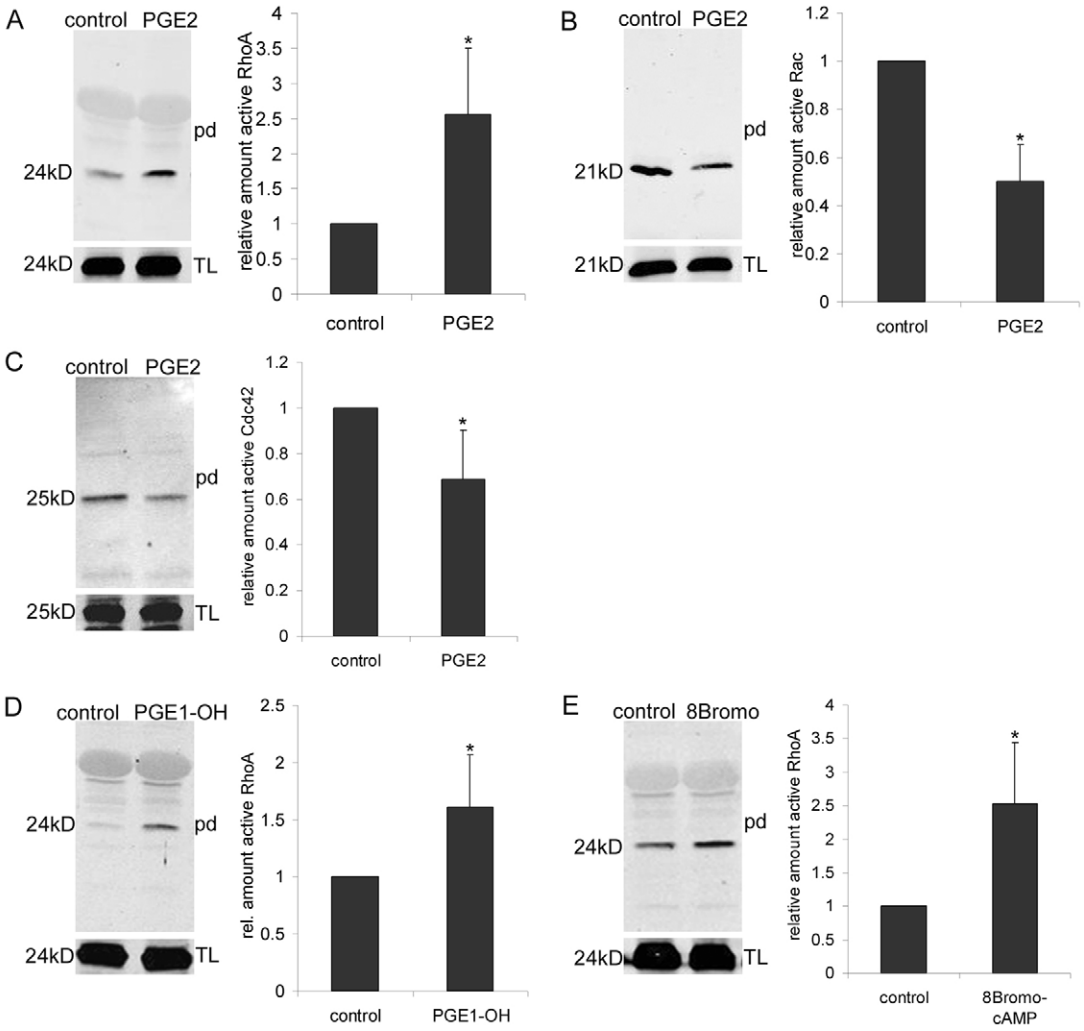

Fig. 6. PGE_2-receptor stimulation leads to activation of RhoA and inactivation of Rac1 and Cdc42. (A) Activation of the small GTPase RhoA in response to PGE_2. GTP-RhoA levels were determined in lysates (pd, pull down; TL, total lysate) of HL-60 cells using a Rhotekin-GST pull-down assay. In cells treated with PGE_2 for 5 minutes, Rho-GTP levels showed a 2.6±0.9 (s.d.)-fold increase relative to untreated cells (n=7). (B) Loss of Rac1 GTPase activity in response to PGE_2. Rac1-GTP levels were determined in lysates of HL-60 cells using a biotinylated Pak1 peptide. In cells stimulated with PGE_2, Rac1 activity was decreased 0.5±0.2 (s.d.)-fold relative to untreated cells (n=6). (C) Loss of Cdc42 GTPase activity in response to PGE_2. Cdc42-GTP levels were determined in lysates of HL-60 cells using a biotinylated Pak1 peptide. In cells stimulated with PGE_2, Cdc42 activity was decreased 0.7±0.2 (s.d.)-fold relative to untreated cells (n=6). (D,E) Activation of the small GTPase RhoA in response to PGE_1-OH or 8-Bromo-cAMP. GTP-RhoA levels were determined in lysates of HL-60 cells using a Rhotekin-GST pull-down assay. (D) In cells treated for 5 minutes with an EP4 agonist (PGE_1-OH), Rho-GTP levels showed a 1.6±0.5 (s.d.)-fold increase relative to untreated cells (n=8). (E) In cells treated for 5 minutes with 8-Bromo-cAMP (8Bromo, 200 μM), which elevates cAMP levels, Rho-GTP levels showed a 2.5±0.9 (s.d.)-fold increase relative to untreated cells (n=5). Asterisks indicate significant differences (P<0.05).

expression of EP2/EP4 but not EP1/EP3 was detected in DCs. The effects of specific EP4-(ant)agonists implicate this receptor in PGE_2-induced podosome loss. Similarly, the effects of a specific EP2 agonist and the lack thereof in response to an EP1/EP3 agonist similarly support a role for the EP2 receptor in PGE_2-mediated podosome loss. These pharmacological studies, combined with the observed expression pattern, suggest that these PGE_2-induced responses in DCs are mediated by EP2/EP4 receptors, both of which signal through G_s to elevate cAMP levels (Narumiya and FitzGerald, 2001). Indeed, we observed that raising cAMP levels mimics the effects of PGE_2 on podosome dissolution.

Although podosome formation has been studied in some detail, much less is known about signalling mechanisms that trigger podosome dissolution. Small GTPases of the Rho family (RhoA, Rac1 and Cdc42) are key regulators of adhesion dynamics that control the formation and turnover of filamentous actin as well as microtubules, and modulate myosin-II-based contractility (Burridge and Wennerberg, 2004; De la Roche et al., 2002). In endothelial cells, podosome organization is regulated by RhoA and Cdc42 (Moreau et al., 2003), and in Src-transformed fibroblasts, active RhoA localizes to podosomes (Berdeaux et al., 2004). Inhibition of RhoA maintains the podosome belt at the osteoclast periphery despite depolymerization of microtubules by nocodazole (Destaing et al., 2005), suggesting that RhoA activity is needed to induce podosome loss. Consistent with these observations in osteoclasts, we found that PGE_2-induced podosome dissolution involves activation of RhoA. Ourselves and others have shown that activation of RhoA is often accompanied by a loss of Rac1 activity, whereas active forms of these two Rho GTPases often produce opposite effects on the cytoskeleton (Price et al., 1998; Van

Leeuwen et al., 1997). Indeed, PGE_2-mediated activation of RhoA is accompanied by a decrease in activity of both Rac1 and Cdc42. It has previously been shown that Rac1 as well as Cdc42 are needed for podosome formation in DCs (Burns et al., 2001), whereas the Cdc42/Rac1-regulated kinases Pak1 and Pak4 either induce podosome formation or reduce podosome turnover (Gringel et al., 2006; Webb et al., 2005; Webb et al., 2002). Another effector of Cdc42, the Wiskott-Aldrich syndrome protein (WASp), also plays an essential role in the formation and maintenance of podosomes in both human macrophages (Linder et al., 1999) and endothelial cells (Moreau et al., 2003), whereas WASp-deficient DCs and macrophages lack podosomes (Burns et al., 2004; Linder et al., 1999). Together, these data suggest that PGE_2-mediated activation of RhoA combined with a simultaneous inactivation of Rac1 and Cdc42 contribute to the dissolution of podosomes in DCs and HL-60 cells.

In most cell types, cAMP-mediated activation of PKA antagonizes the effects of RhoA on actomyosin contractility, leading to cytoskeletal relaxation (Dong et al., 1998; Lang et al., 1996; Manganello et al., 2003). In DCs, however, PGE_2 stimulation appears to induce a contractile response while activating RhoA. Similar to PGE_2, we observed cytoskeletal contraction and increased RhoA-GTP levels in response to EP agonists as well as to stimulation with the cAMP analogue 8-Bromo-cAMP. In addition, stimulation with a PKA activator resulted in increased levels of RhoA-GTP in HL-60 cells, whereas PKA inhibition interfered with PGE_2-induced podosome loss in DCs (data not shown). Together, these results indicate that activation of RhoA as well as PGE_2-induced podosome dissolution is mediated by cAMP-PKA signalling.

In most adherent cells, the formation of stress fibres and stable FAs is triggered by activation of RhoA and its downstream effector Rho kinase, promoting actomyosin contractility (Burridge and Wennerberg, 2004). Rho kinase acts by promoting phosphorylation of the myosin II regulatory light chain (Amano et al., 1996; Kimura et al., 1996). In addition, Rho-kinase activity can enhance stress fibre formation by inactivation of the actin-severing protein cofilin (Maekawa et al., 1999), whereas direct activation of mDia by RhoA stimulates actin polymerization (Burridge and Wennerberg, 2004; Geneste et al., 2002). Therefore, we assessed the effects of Rho-kinase inhibition on PGE_2-induced podosome dissolution. In smooth muscle cells, phorbol-dibutyrate-induced podosome formation appears to be Rho-kinase independent (Hai et al., 2002). In our experiments, however, inhibition of Rho kinase not only effectively interfered with podosome dissolution induced by PGE_2, but also

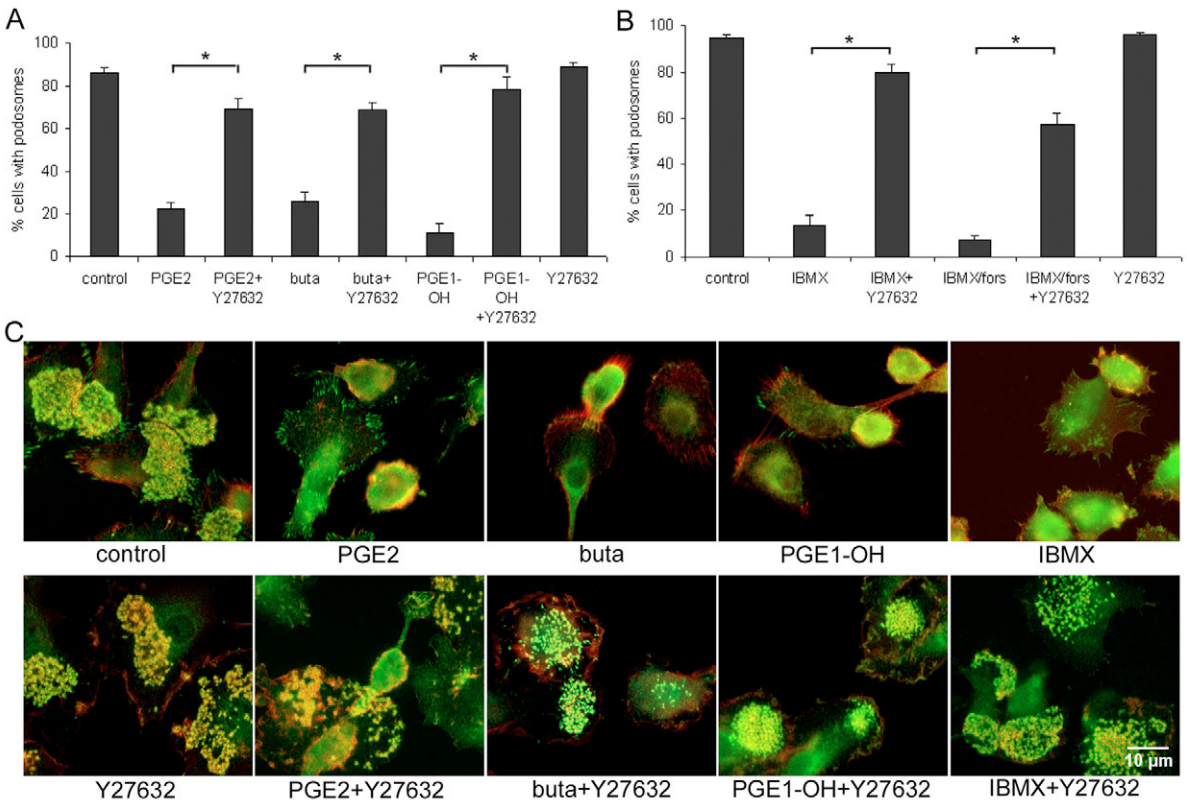

Fig. 7. Podosome loss induced by PGE_2, EP agonists and elevated cAMP is mediated by Rho kinase. (A) Rho-kinase inhibition blocks PGE_2- and EP-agonist-induced podosome dissolution. iDCs seeded on FN-coated coverslips were left untreated or were stimulated with PGE_2 (for 5 minutes), butaprost (buta, 2 µM for 15 minutes) or PGE_1-OH (5 µg/ml for 30 minutes), in the presence or absence of Y27632 (20 µM for 1 hour), or were treated with Y27632 alone, and stained with anti-vinculin mAb and phalloidin-Texas Red (to detect F-actin). The number of cells displaying podosomes was determined in seven images per condition per experiment and an average (with s.e.m.) of three experiments is shown. (B) IBMX and IBMX/forskolin-induced podosome dissolution is efficiently blocked by Y27632. iDCs seeded on FN-coated coverslips were left untreated or were stimulated with IBMX (10 µM for 5 minutes) or IBMX with forskolin (IBMX/fors, both 10 µM for 5 minutes) in the presence or absence of Y27632 (20 µM for 1 hour), or with Y27632 alone, and stained with anti-vinculin mAb and phalloidin-Texas Red (to detect F-actin). The number of cells displaying podosomes was counted in seven images per condition per experiment and an average (with s.e.m.) of three experiments is shown. Asterisks indicate significant differences (P<0.05). (C) Rho-kinase inhibition blocks podosome loss in response to PGE_2, EP2/EP4 agonists or cAMP elevation. Representative images are depicted.

interfered with that induced by EP agonists and by elevated cAMP levels. This effect of Rho kinase was observed in primary DCs as well as in HL-60 cells, demonstrating that PGE_2-induced podosome dissolution is dependent on Rho-kinase activity both in DCs and these monocytic leukaemia cells. This is the first demonstration that (camp-elevating) EP2/EP4 receptors can signal to activate the RhoA–Rho-kinase axis, and our results indicate that inhibition of RhoA signalling downstream of cAMP is not a universal principle.

A number of studies have implicated myosin II in podosome regulation. For instance, formation of podosomes was shown to involve (local) inhibition of myosin II in smooth muscle cells as well as neuroblastoma cells (Burgstaller and Gimona, 2004; Clark et al., 2006), whereas, in macrophages (Kopp et al., 2006) or fibroblasts (Collin et al., 2006), myosin-II-based activity is needed for the formation and maintenance of these structures.

Although these different experimental outcomes might be in part dependent on cell type or culture conditions, we propose that basal myosin IIA activity is required for the formation and maintenance of podosomes, whereas a sudden (stimulus-induced) increase in myosin II activity might trigger podosome dissolution. This idea is supported by our findings that relatively low concentrations of blebbistatin (10 μM) effectively block PGE_2-induced podosome loss without affecting podosome turnover, whereas higher concentrations (40-100 μM) interfere with the formation and/or maintenance of these structures (Collin et al., 2006; Kopp et al., 2006). Hence, we conclude that, dependent on cell type and experimental conditions, local changes in myosin II activity can either trigger the formation of podosomes or contribute to their demise.

In mammalian cells, three myosin II isoforms have been identified, known as myosin IIA, myosin IIB and myosin IIC (Golomb et al., 2004; Katsuragawa et al., 1989; Shohet et al., 1989). Here, we show that myosin IIA, the predominant isoform expressed in DCs, localizes to podosome rings, whereas only trace amounts of myosin IIB are present. Although we cannot exclude a role for myosin IIB in podosome dissolution in DCs, the prominent expression and localization of myosin IIA to podosome-rich areas of the cells suggests that this myosin isoform is primarily involved in PGE_2-mediated podosome dissolution. Pharmacological inhibition of myosin II function, using blebbistatin, demonstrated a requirement for myosin II in PGE_2-induced podosome dissolution. In addition, PGE_2 stimulation in DCs leads to a noticeable change in myosin II distribution, from a punctuate cytosolic pattern to a more fibrillar distribution. These fibrillar structures are reminiscent of the myosin II ribbons described in fibroblasts (Verkhovsky et al., 1995) and most likely reflect increased association with F-actin and/or a change in solubility of myosin filaments.

We have shown previously, in mouse neuroblastoma cells, that pharmacological inhibition of myosin II leads to a loss of focal adhesions accompanied by the formation of podosomes (Clark et al., 2006). In addition, WASp-interacting-protein-deficient DCs lack podosomes, but still form FAs (Chou et al., 2006). Furthermore, in avian multinucleated giant cells, disruption of the microtubules by nocodazole induced the loss of podosomes accompanied by the formation of stress fibres and FAs, and activation of RhoA and inactivation of Rac1, whereas repolymerization of microtubules induced the loss of FAs and reformation of podosomes (Ory et al., 2002). These findings suggest that, in different cell types, podosomes and FAs are oppositely affected by Rho GTPase activity and actomyosin contractility. Hence, we propose that localized changes in actin dynamics in combination with the contractile state of a cell determine whether FAs or podosomes are formed.

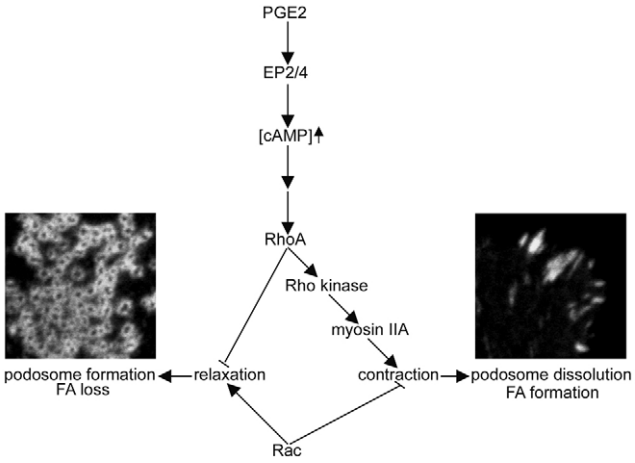

Fig. 8. Regulation of adhesion dynamics in dendritic cells by PGE_2. PGE_2 signalling, mediated by EP2 and EP4 receptors, leads to elevation of the level of cAMP, activation of RhoA and inactivation of Rac1. PGE_2-mediated activation of RhoA promotes Rho-kinase activity and, subsequently, myosin-II-dependent contraction, leading to podosome dissolution and FA formation. By contrast, pathways leading to activation of Rac1 are known to promote podosome formation and induce cytoskeletal relaxation accompanied by a loss of FAs.

Besides enabling high-speed migration, PGE_2-induced podosome dissolution could have additional functions. It might serve to redeploy actin to other processes in the cell, such as vesicle movement, which has been linked to podosome dynamics (Cougoule et al., 2005; McNiven et al., 2004). Furthermore, microtubules were shown to influence FA and podosome dynamics, an effect that could be mediated by (microtubule-dependent) vesicle transport (Ezratty et al., 2005; Kopp et al., 2006). In mouse DCs, a loss of podosomes was associated with a transient increase in antigen uptake (West et al., 2004). Similarly, we observed a moderate increase in antigen uptake in human DCs shortly after stimulation with PGE_2 (data not shown). Thus, in addition to enabling high-speed migration, podosome dissolution in DCs could transiently enhance antigen uptake and thereby add to the induction of immune responses.

As summarized in the model shown in Fig. 8, our data show that PGE_2 mediates podosome dissolution by myosin-II-mediated contractility downstream of RhoA and Rho-kinase activation. This is the first report showing activation of the RhoA–Rho-kinase axis downstream of receptors (EP2/EP4) known to couple to cAMP elevation. Moreover, our data provide novel insights into the dynamics of the DC cytoskeleton and its regulation during the induction of DC maturation.

Materials and Methods

Chemicals and antibodies

Antibodies used were: mIgG1 (Becton Dickinson and Company), GaM-ATTO633, anti-vinculin and anti-myosin IIB (Sigma), anti-myosin IIA (Biomedical Technologies), anti-myosin IIC [obtained from R. Adelstein, National Institutes of Health (NIH), Bethesda, MD], anti-RhoA and anti-zyxin (Santa Cruz Biotechnology), anti-Rac1 (Upstate Biotechnology, Millipore), IRDye 800 CW-labelled secondary antibodies (LI-COR Biosciences), and Alexa-Fluor-488-labeled secondary antibodies and Texas Red-conjugated phalloidin (Molecular Probes).

Chemicals used were: blebbistatin, Y27632 and PMA (Calbiochem), FN, butaprost, sulprostone, AH23848, AH6809, IBMX, forskolin and 8-Bromo-cAMP (Sigma), and PGE_1-OH (Cayman Chemical Company). PGE_2 was used at 10 μg/ml (Pharmacia & Upjohn).

Isolation of monocytes, preparation of DCs and cell culture

DCs were generated from peripheral blood mononuclear cells as described previously (De Vries et al., 2003a). Expression of major histocompatibility complex class I/II, co-stimulatory molecules and DC-specific markers were measured by flow cytometry on iDCs d6 and expression was similar to what was described before (data not shown) (De Vries et al., 2003a). HL-60 cells (generous gift from L. Machesky, CRUK Beatson Institute for Cancer Research, Glasgow, Scotland) were cultured in IMDM medium (Invitrogen) supplemented with 10% (v/v) FCS (Greiner). N1E-115 cells were cultured in DMEM medium (Invitrogen) supplemented with 10% (v/v) FCS.

Fluorescence microscopy

Fluorescence microscopy was performed as described previously (Van Helden et al., 2006). A Leica DMRA fluorescence microscope with 63× PL APO 1.3 NA or 40× PL FLUOTAR 1.0 NA oil-immersion lens and COHU high-performance integrating CCD camera were used. Pictures were analyzed with Leica Qfluoro version V1.2.0 and Adobe Photoshop 7.0 software.

Interference reflection microscopy (IRM)

IRM was performed using a Zeiss LSM 510-meta microscope with 488-nm laser with a band-pass filter at 470-500 nm, or a 633-nm laser with a long-pass filter at 560 nm and a Plan-Apochromatic 63× 1.4 NA oil-immersion DIC lens (Carl Zeiss GmbH). Cells were seeded on FN-coated Willco glass-bottom dishes (Willco Wells BV), and either fixed and stained for vinculin and actin before fluorescent and IRM images were obtained, or cells were live-imaged in IRM mode with 20-second intervals at 37°C in RPMI 1640 without phenol red (Invitrogen) during addition of PGE_2. In addition, cells were live-imaged in IRM mode and fixed while podosomes were dissolving upon PGE_2 stimulation, and stained for actin and vinculin, myosin IIA or zyxin, and fluorescent and IRM images were obtained. Cells were imaged using Zeiss LSM Image Browser version 32 and images were processed with ImageJ version 1.32j software (National Institutes of Health, http://rsb.info.nih.gov/ij).

RT-PCR

RNA was isolated from iDCs, mDCs and HL-60 cells with Trizol reagent (Gibco) according to the instruction of the manufacturer. An RT-PCR was performed using a T3 thermocycler at 20°C for 10 minutes, 42°C for 45 minutes and 95°C for 10 minutes. An annealing temperature of 55°C with 30 cycles was used. The following primers were used: EP1 forward, 5′-ATCATGGTGGTGTCGTGCATC-3′; EP1 reverse, 5′-GGTCCAGGATCTGGTTCCAG-3′; EP2 forward, 5′-ATGACCATC-ACCTTCGCC-3′; EP2 reverse, 5′-CAAAGACCCAAGGGTCAATT-3′; EP3 forward, 5′-GTATGCGAGCCACATGAAG A-3′; EP3 reverse, 5′-CAGAGG-CGAAGAAAAGGTTG-3′; EP4 forward, 5′-TCCTGGCTT TTGAGCACTTT-3′; EP4 reverse, 5′-CCTCTGCTGTGTGCCAAATA-3′; actin forward, 5′-GCTAC-GAGCTGCCTGACGG-3′; actin reverse, 5′-GAGGCCAGGATGGAGCC-3′.

RhoA-, Rac1- and Cdc42-activation assay and myosin II isoform detection

RhoA, Rac1 and Cdc42 pull-down experiments were performed as described previously (Van Leeuwen et al., 2003). Samples were analyzed by western blotting using mouse anti-RhoA or anti-Rac1 antibodies, or a rabbit anti-Cdc42 antibody. Cell lysates were analyzed for myosin II isoform expression by western blotting using rabbit anti-myosin IIA, -myosin IIB or -myosin IIC antibodies. Samples were analyzed on an Odyssey infrared imaging system (LI-COR Biosciences).

Statistical analysis

ANOVA or the two-tailed *t*-test were used for statistical analysis. Significant differences or significant differences from control are indicated with asterisks ($P<0.05$).

We thank L. Machesky for providing the HL-60 cells and R. Adelstein for providing myosin IIC antibodies. We thank I. de Vries, N. Meeuwsen-Scharenborg, A. de Boer, M. van de Rakt and M. Kerkhoff for providing DCs. This study was supported by research funding from the Foundation for Fundamental Research on Matter (FOM 01FB06) and the Dutch Cancer Society (KWF KUN 2006-3699).

References

Abramovitz, M., Adam, M., Boie, Y., Carriere, M., Denis, D., Godbout, C., Lamontagne, S., Rochette, C., Sawyer, N., Tremblay, N. M. et al. (2000). The utilization of recombinant prostanoid receptors to determine the affinities and selectivities of prostaglandins and related analogs. *Biochim. Biophys. Acta* **1483**, 285-293.

Amano, M., Ito, M., Kimura, K., Fukata, Y., Chihara, K., Nakano, T., Matsuura, Y. and Kaibuchi, K. (1996). Phosphorylation and activation of myosin by Rho-associated kinase (Rho-kinase). *J. Biol. Chem.* **271**, 20246-20249.

Banchereau, J. and Steinman, R. M. (1998). Dendritic cells and the control of immunity. *Nature* **392**, 245-252.

Berdeaux, R. L., Diaz, B., Kim, L. and Martin, G. S. (2004). Active Rho is localized to podosomes induced by oncogenic Src and is required for their assembly and function. *J. Cell Biol.* **166**, 317-323.

Blaschke, V., Jungermann, K. and Puschel, G. P. (1996). Exclusive expression of the Gs-linked prostaglandin E2 receptor subtype 4 mRNA in mononuclear Jurkat and KM-3 cells and coexpression of subtype 4 and 2 mRNA in U-937 cells. *FEBS Lett.* **394**, 39-43.

Buccione, R., Orth, J. D. and McNiven, M. A. (2004). Foot and mouth: podosomes, invadopodia and circular dorsal ruffles. *Nat. Rev. Mol. Cell Biol.* **5**, 647-657.

Burgstaller, G. and Gimona, M. (2004). Actin cytoskeleton remodelling via local inhibition of contractility at discrete microdomains. *J. Cell Sci.* **117**, 223-231.

Burns, S., Thrasher, A. J., Blundell, M. P., Machesky, L. and Jones, G. E. (2001). Configuration of human dendritic cell cytoskeleton by Rho GTPases, the WAS protein, and differentiation. *Blood* **98**, 1142-1149.

Burns, S., Hardy, S. J., Buddle, J., Yong, K. L., Jones, G. E. and Thrasher, A. J. (2004). Maturation of DC is associated with changes in motile characteristics and adherence. *Cell Motil. Cytoskeleton* **57**, 118-132.

Burridge, K. and Wennerberg, K. (2004). Rho and Rac take center stage. *Cell* **116**, 167-179.

Calle, Y., Carragher, N. O., Thrasher, A. J. and Jones, G. E. (2006). Inhibition of calpain stabilises podosomes and impairs dendritic cell motility. *J. Cell Sci.* **119**, 2375-2385.

Carman, C. V., Sage, P. T., Sciuto, T. E., de la Fuente, M. A., Geha, R. S., Ochs, H. D., Dvorak, H. F., Dvorak, A. M. and Springer, T. A. (2007). Transcellular diapedesis is initiated by invasive podosomes. *Immunity* **26**, 784-797.

Chou, H. C., Anton, I. M., Holt, M. R., Curcio, C., Lanzardo, S., Worth, A., Burns, S., Thrasher, A. J., Jones, G. E. and Calle, Y. (2006). WIP regulates the stability and localization of WASP to podosomes in migrating dendritic cells. *Curr. Biol.* **16**, 2337-2344.

Clark, K., Langeslag, M., van Leeuwen, B., Ran, L., Ryazanov, A. G., Figdor, C. G., Moolenaar, W. H., Jalink, K. and van Leeuwen, F. N. (2006). TRPM7, a novel regulator of actomyosin contractility and cell adhesion. *EMBO J.* **25**, 290-301.

Collin, O., Tracqui, P., Stephanou, A., Usson, Y., Clement-Lacroix, J. and Planus, E. (2006). Spatiotemporal dynamics of actin-rich adhesion microdomains: influence of substrate flexibility. *J. Cell Sci.* **119**, 1914-1925.

Cougoule, C., Carreno, S., Castandet, J., Labrousse, A., Astarie-Dequeker, C., Poincloux, R., Le Cabec, V. and Maridonneau-Parini, I. (2005). Activation of the lysosome-associated p61Hck isoform triggers the biogenesis of podosomes. *Traffic* **6**, 682-694.

De la Roche, M. A., Smith, J. L., Betapudi, V., Egelhoff, T. T. and Cote, G. P. (2002). Signaling pathways regulating Dictyostelium myosin II. *J. Muscle Res. Cell Motil.* **23**, 703-718.

De Vries, I. J., Krooshoop, D. J., Scharenborg, N. M., Lesterhuis, W. J., Diepstra, J. H., Van Muijen, G. N., Strijk, S. P., Ruers, T. J., Boerman, O. C., Oyen, W. J. et al. (2003a). Effective migration of antigen-pulsed dendritic cells to lymph nodes in melanoma patients is determined by their maturation state. *Cancer Res.* **63**, 12-17.

De Vries, I. J., Lesterhuis, W. J., Scharenborg, N. M., Engelen, L. P., Ruiter, D. J., Gerritsen, M. J., Croockewit, S., Britten, C. M., Torensma, R., Adema, G. J. et al. (2003b). Maturation of dendritic cells is a prerequisite for inducing immune responses in advanced melanoma patients. *Clin. Cancer Res.* **9**, 5091-5100.

Destaing, O., Saltel, F., Geminard, J. C., Jurdic, P. and Bard, F. (2003). Podosomes display actin turnover and dynamic self-organization in osteoclasts expressing actin-green fluorescent protein. *Mol. Biol. Cell* **14**, 407-416.

Destaing, O., Saltel, F., Gilquin, B., Chabadel, A., Khochbin, S., Ory, S. and Jurdic, P. (2005). A novel Rho-mDia2-HDAC6 pathway controls podosome patterning through microtubule acetylation in osteoclasts. *J. Cell Sci.* **118**, 2901-2911.

Dong, J. M., Leung, T., Manser, E. and Lim, L. (1998). cAMP-induced morphological changes are counteracted by the activated RhoA small GTPase and the Rho kinase ROKalpha. *J. Biol. Chem.* **273**, 22554-22562.

Ezratty, E. J., Partridge, M. A. and Gundersen, G. G. (2005). Microtubule-induced focal adhesion disassembly is mediated by dynamin and focal adhesion kinase. *Nat. Cell Biol.* **7**, 581-590.

Geneste, O., Copeland, J. W. and Treisman, R. (2002). LIM kinase and Diaphanous cooperate to regulate serum response factor and actin dynamics. *J. Cell Biol.* **157**, 831-838.

Golomb, E., Ma, X., Jana, S. S., Preston, Y. A., Kawamoto, S., Shoham, N. G., Goldin, E., Conti, M. A., Sellers, J. R. and Adelstein, R. S. (2004). Identification and characterization of nonmuscle myosin II-C, a new member of the myosin II family. *J. Biol. Chem.* **279**, 2800-2808.

Gringel, A., Walz, D., Rosenberger, G., Minden, A., Kutsche, K., Kopp, P. and Linder, S. (2006). PAK4 and alphaPIX determine podosome size and number in macrophages through localized actin regulation. *J. Cell. Physiol.* **209**, 568-579.

Hai, C. M., Hahne, P., Harrington, E. O. and Gimona, M. (2002). Conventional protein kinase C mediates phorbol-dibutyrate-induced cytoskeletal remodeling in a7r5 smooth muscle cells. *Exp. Cell Res.* **280**, 64-74.

Harizi, H., Grosset, C. and Gualde, N. (2003). Prostaglandin E2 modulates dendritic cell function via EP2 and EP4 receptor subtypes. *J. Leukoc. Biol.* **73**, 756-763.

Hata, A. N. and Breyer, R. M. (2004). Pharmacology and signaling of prostaglandin receptors: multiple roles in inflammation and immune modulation. *Pharmacol Ther.* **103**, 147-166.

Kabashima, K., Sakata, D., Nagamachi, M., Miyachi, Y., Inaba, K. and Narumiya, S. (2003). Prostaglandin E2-EP4 signaling initiates skin immune responses by promoting migration and maturation of Langerhans cells. *Nat. Med.* **9**, 744-749.

Katsuragawa, Y., Yanagisawa, M., Inoue, A. and Masaki, T. (1989). Two distinct nonmuscle myosin-heavy-chain mRNAs are differentially expressed in various chicken tissues. Identification of a novel gene family of vertebrate non-sarcomeric myosin heavy chains. *Eur. J. Biochem.* **184**, 611-616.

Kaverina, I., Stradal, T. E. and Gimona, M. (2003). Podosome formation in cultured A7r5 vascular smooth muscle cells requires Arp2/3-dependent de-novo actin polymerization at discrete microdomains. *J. Cell Sci.* **116**, 4915-4924.

Kimura, K., Ito, M., Amano, M., Chihara, K., Fukata, Y., Nakafuku, M., Yamamori, B., Feng, J., Nakano, T., Okawa, K. et al. (1996). Regulation of myosin phosphatase by Rho and Rho-associated kinase (Rho-kinase). *Science* **273**, 245-248.

Kopp, P., Lammers, R., Aepfelbacher, M., Woehlke, G., Rudel, T., Machuy, N., Steffen, W. and Linder, S. (2006). The kinesin KIF1C and microtubule plus ends regulate podosome dynamics in macrophages. *Mol. Biol. Cell* **17**, 2811-2823.

Lang, P., Gesbert, F., Delespine-Carmagnat, M., Stancou, R., Pouchelet, M. and Bertoglio, J. (1996). Protein kinase A phosphorylation of RhoA mediates the morphological and functional effects of cyclic AMP in cytotoxic lymphocytes. *EMBO J.* **15**, 510-519.

Legler, D. F., Krause, P., Scandella, E., Singer, E. and Groettrup, M. (2006). Prostaglandin E2 is generally required for human dendritic cell migration and exerts its effect via EP2 and EP4 receptors. *J. Immunol.* **176**, 966-973.

Linder, S. and Aepfelbacher, M. (2003). Podosomes: adhesion hot-spots of invasive cells. *Trends Cell Biol.* **13**, 376-385.

Linder, S., Nelson, D., Weiss, M. and Aepfelbacher, M. (1999). Wiskott-Aldrich syndrome protein regulates podosomes in primary human macrophages. *Proc. Natl. Acad. Sci. USA* **96**, 9648-9653.

Maekawa, M., Ishizaki, T., Boku, S., Watanabe, N., Fujita, A., Iwamatsu, A., Obinata, T., Ohashi, K., Mizuno, K. and Narumiya, S. (1999). Signaling from Rho to the actin cytoskeleton through protein kinases ROCK and LIM-kinase. *Science* **285**, 895-898.

Manganello, J. M., Huang, J. S., Kozasa, T., Voyno-Yasenetskaya, T. A. and Le Breton, G. C. (2003). Protein kinase A-mediated phosphorylation of the Galpha13 switch I region alters the Galphabetagamma13-G protein-coupled receptor complex and inhibits Rho activation. *J. Biol. Chem.* **278**, 124-130.

McNiven, M. A., Baldassarre, M. and Buccione, R. (2004). The role of dynamin in the assembly and function of podosomes and invadopodia. *Front. Biosci.* **9**, 1944-1953.

Mellman, I., Turley, S. J. and Steinman, R. M. (1998). Antigen processing for amateurs and professionals. *Trends Cell Biol.* **8**, 231-237.

Moreau, V., Tatin, F., Varon, C. and Genot, E. (2003). Actin can reorganize into podosomes in aortic endothelial cells, a process controlled by Cdc42 and RhoA. *Mol. Cell. Biol.* **23**, 6809-6822.

Narumiya, S. and FitzGerald, G. A. (2001). Genetic and pharmacological analysis of prostanoid receptor function. *J. Clin. Invest.* **108**, 25-30.

Ory, S., Destaing, O. and Jurdic, P. (2002). Microtubule dynamics differentially regulates Rho and Rac activity and triggers Rho-independent stress fiber formation in macrophage polykaryons. *Eur. J. Cell Biol.* **81**, 351-362.

Price, L. S., Leng, J., Schwartz, M. A. and Bokoch, G. M. (1998). Activation of Rac and Cdc42 by integrins mediates cell spreading. *Mol. Biol. Cell* **9**, 1863-1871.

Rubio, M. T., Means, T. K., Chakraverty, R., Shaffer, J., Fudaba, Y., Chittenden, M., Luster, A. D. and Sykes, M. (2005). Maturation of human monocyte-derived dendritic cells (MoDCs) in the presence of prostaglandin E2 optimizes CD4 and CD8 T cell-mediated responses to protein antigens: role of PGE2 in chemokine and cytokine expression by MoDCs. *Int. Immunol.* **17**, 1561-1572.

Scandella, E., Men, Y., Gillessen, S., Forster, R. and Groettrup, M. (2002). Prostaglandin E2 is a key factor for CCR7 surface expression and migration of monocyte-derived dendritic cells. *Blood* **100**, 1354-1361.

Shohet, R. V., Conti, M. A., Kawamoto, S., Preston, Y. A., Brill, D. A. and Adelstein, R. S. (1989). Cloning of the cDNA encoding the myosin heavy chain of a vertebrate cellular myosin. *Proc. Natl. Acad. Sci. USA* **86**, 7726-7730.

Straight, A. F., Cheung, A., Limouze, J., Chen, I., Westwood, N. J., Sellers, J. R. and Mitchison, T. J. (2003). Dissecting temporal and spatial control of cytokinesis with a myosin II Inhibitor. *Science* **299**, 1743-1747.

Uehata, M., Ishizaki, T., Satoh, H., Ono, T., Kawahara, T., Morishita, T., Tamakawa, H., Yamagami, K., Inui, J., Maekawa, M. et al. (1997). Calcium sensitization of smooth muscle mediated by a Rho-associated protein kinase in hypertension. *Nature* **389**, 990-994.

Usson, Y., Guignandon, A., Laroche, N., Lafage-Proust, M. H. and Vico, L. (1997). Quantitation of cell-matrix adhesion using confocal image analysis of focal contact associated proteins and interference reflection microscopy. *Cytometry* **28**, 298-304.

Van Helden, S. F., Krooshoop, D. J., Broers, K. C., Raymakers, R. A., Figdor, C. G. and van Leeuwen, F. N. (2006). A critical role for prostaglandin E2 in podosome dissolution and induction of high-speed migration during dendritic cell maturation. *J. Immunol.* **177**, 1567-1574.

Van Leeuwen, F. N., Kain, H. E., Kammen, R. A., Michiels, F., Kranenburg, O. W. and Collard, J. G. (1997). The guanine nucleotide exchange factor Tiam1 affects neuronal morphology; opposing roles for the small GTPases Rac and Rho. *J. Cell Biol.* **139**, 797-807.

Van Leeuwen, F. N., Olivo, C., Grivell, S., Giepmans, B. N., Collard, J. G. and Moolenaar, W. H. (2003). Rac activation by lysophosphatidic acid LPA1 receptors through the guanine nucleotide exchange factor Tiam1. *J. Biol. Chem.* **278**, 400-406.

Verkhovsky, A. B., Svitkina, T. M. and Borisy, G. G. (1995). Myosin II filament assemblies in the active lamella of fibroblasts: their morphogenesis and role in the formation of actin filament bundles. *J. Cell Biol.* **131**, 989-1002.

Webb, B. A., Eves, R., Crawley, S. W., Zhou, S., Cote, G. P. and Mak, A. S. (2005). PAK1 induces podosome formation in A7r5 vascular smooth muscle cells in a PAK-interacting exchange factor-dependent manner. *Am. J. Physiol. Cell. Physiol.* **289**, C898-C907.

Webb, D. J., Parsons, J. T. and Horwitz, A. F. (2002). Adhesion assembly, disassembly and turnover in migrating cells - over and over and over again. *Nat. Cell Biol.* **4**, E97-E100.

West, M. A., Wallin, R. P., Matthews, S. P., Svensson, H. G., Zaru, R., Ljunggren, H. G., Prescott, A. R. and Watts, C. (2004). Enhanced dendritic cell antigen capture via toll-like receptor-induced actin remodeling. *Science* **305**, 1153-1157.

Zaidel-Bar, R., Ballestrem, C., Kam, Z. and Geiger, B. (2003). Early molecular events in the assembly of matrix adhesions at the leading edge of migrating cells. *J. Cell Sci.* **116**, 4605-4613.

Zamir, E. and Geiger, B. (2001). Molecular complexity and dynamics of cell-matrix adhesions. *J. Cell Sci.* **114**, 3583-3590.